

Extrapolation Properties of the Chebyshev Polynomial Expansion Potential

A. SINANAJ AND A. PASHOV*

Faculty of Physics, Sofia University, bul. J. Bourchier 5, 1164 Sofia, Bulgaria

Received: 21.08.2024 & Accepted: 02.09.2024

Doi: [10.12693/APhysPolA.146.259](https://doi.org/10.12693/APhysPolA.146.259)

*e-mail: pashov@phys.uni-sofia.bg

Finding analytic functions capable of representing various potential curves for diatomic molecules is one of the important problems in spectroscopy. The ability to properly represent the form of the potential curve at large internuclear distances is particularly valuable. In this paper, we study the extrapolation properties of the Chebyshev polynomial expansion, reported by V.V. Meshkov and co-authors in *J. Chem. Phys.* **140**, 064315 (2014). Among its many useful features, this potential form has a built-in asymptote, $U_\infty - C_6/R^6 - C_8/R^8 - \dots$, so it is plausible to expect that the dispersion coefficients can be obtained by fitting the Chebyshev polynomial expansion form to the experimental data.

topics: diatomic molecules, potential energy curves, dispersion coefficients, extrapolation properties

1. Introduction

The potential energy curve is an important part of physical problems, the solution of which can be reduced to the one-dimensional Schrödinger equation. Such are the energy levels of diatomic molecules, treated within the Born–Oppenheimer approximation. Very often this approximation is well justified (even in high-resolution studies) for isolated electronic states, whose potential curves (PECs) are energetically separated and do not cross. But even in the case of potential curves crossing, the energy levels can be modeled by a set of coupled Schrödinger equations, where the zero-order Born–Oppenheimer PECs play the same important role.

Being an unobservable object, the PEC can not be measured experimentally. It can be calculated by solving the multidimensional Schrödinger equation (SE) for electrons by fixed nuclei, but this approach can very rarely reach experimental accuracy despite the tremendous improvement in modern *ab initio* calculations. A more accurate approach is to treat the PEC as an empirical object and to fit it to the experimental data — the so-called inverse problem. Before the widely available powerful computers, this problem was solved analytically within a semi-classical approximation by Rydberg, Klein, and Rees [1–3]. The solution, the so-called RKR curve, is obtained in a point-wise form (R_i, U_i), where the highest energy U_{\max} is equal to the highest observed level energy. It is beyond the scope of the present paper to review all the properties of

the RKR potentials; it is sufficient to say that although being moderately accurate (compared to *ab initio* curves), these potentials lack any extrapolation properties. After the pioneering works of Kosman and Hinze [4] and Vidal and Scheingraber [5], a fully quantum mechanical method of solving the inverse problem was introduced — the inverted perturbation approach (IPA). Since then, it has been successfully implemented in many computer routines [6–12]. The IPA potentials are by their nature accurate, i.e., through the radial SE, they reproduce the experimental data within their uncertainty. However, the problem with extrapolation properties is not solved automatically by the IPA, because in this method only agreement between experiment and calculated energies is searched. As a rule of thumb, the empirical IPA curve is accurate within the region covered by the experimental data (see Fig. 1).

To speak about extrapolation properties of a PEC, it is necessary to search for an analytic function of R , $U(R, \mathbf{a})$, parametrized by a set of parameters \mathbf{a} . Within the inverse problem, \mathbf{a} are fitted based on experimental information about only part of the PEC (Fig. 1). We speak about good extrapolation properties of a PEC, when \mathbf{a} can be fixed from a limited data set, and the energy levels outside this set can be accurately predicted by the fitted parameters. Unfortunately, accurate analytic model $U(R, \mathbf{a})$ for diatomic molecules, based on general physical considerations, does not exist. There are simple models, like the Morse and Lenard–Jones functions, which are parameterized with a few parameters. These parameters can be

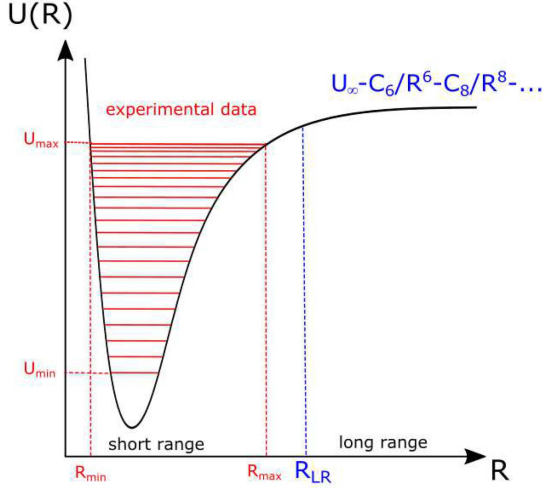


Fig. 1. A scheme of a general potential curve for better understanding of some concepts in this paper. With red lines, experimentally levels are shown and they define the part of the PEC, covered by the following data: $[R_{\min}, R_{\max}]$ — the region of internuclear distances and $[U_{\min}, U_{\max}]$ — the region in energies. The Le Roy radius R_{LR} is shown in blue, and it marks the transition between the short- and the long-range of the potential curve.

fitted from a very small set of experimental data. Still, these models are not accurate, they are not flexible enough to be appropriate even for simple, single-minimum PECs, so their extrapolation properties in most cases are irrelevant. Another extreme are the point-wise cubic-spline potentials (R_i, U_i) [6], where U_i are the fitted parameters. This form is very flexible. It can be used to model not only “regular” single-well PECs [13], but also those with two minima [14], shelf-regions [15], and even more irregular shapes [16]. However, the uncertainty of the parameters U_i that are outside the experimental data increases with energy separation. So, although accurate, this representation cannot predict energy levels very far from the data set used.

Only for a very weakly interacting pair of atoms one can write a simple analytic expression based on the dispersion coefficients C_k [17, 18],

$$U_{LR}(R) = U_{\infty} - \sum_{k=6,8,\dots} \frac{C_k}{R^k}. \quad (1)$$

So, when constructing analytic models with good extrapolation properties, it is desirable to require that they tend to (1) at large internuclear distances. Of course, these properties will only be useful when the experimental data reach the so-called “long-range” region, where (1) becomes valid, so that one can determine the parameters of U_{LR} . No strict definition can be given, but it is estimated to be the region outside the so-called Le Roy radius R_{LR} [18]. The long-range expansion (1) can be attached in a piece-wise manner to existing potential forms, like

in [7, 13]. There, for $R < R_{LR}$ a short-range model is used, while for $R \geq R_{LR}$ — equation (1). Of course, one may require the transition to be continuous and smooth up to some derivative. Alternatively, one may search for a single potential function, such that

$$U(R, \mathbf{a}) \xrightarrow{R \rightarrow \infty} U_{LR}(R). \quad (2)$$

Such forms are, for example, the Morse–Lenard–Jones (MLJ) [6], Morse-long-range (MLR) [19, 20], and Chebyshev polynomial expansion (CPE) [10] potentials. However, having proper asymptotic behavior is not sufficient for the potential form to have good extrapolation properties. This can be understood from the following qualitative considerations. The gradual transition between short- and long-range parts introduces correlations between U_{∞} , C_k , and the rest of the parameters. If the experimental data only reaches the transition region, these correlations may increase the uncertainties of the long-range parameters (thus leading to worse extrapolation). Pure long-range parameters may be fitted only if the experimental data goes deeply into the long-range region. So, the way analytic potential approaches (1) is also important. If it happens too slowly (for $R \gg R_{LR}$), one would need data very close to the dissociation limit to fit the proper long-range parameters, but in such cases, the extrapolations may not be necessary anymore. If the transition happens for $R \ll R_{LR}$, such potentials most likely will not be realistic and flexible enough (like the Lenard–Jones form).

In our recent paper, we studied the extrapolation properties of the MLR potential [21]. For given set of experimental data (about 3500 frequencies of laser-induced lines to the ground X state of Ca_2), we constructed various types of MLR potentials that differ in the number of short-range parameters and in various fixed parameters (details in [21]). It turned out that while the value of the dissociation limit U_{∞} may be fixed quite tightly, the leading dispersion coefficient C_6 may be determined only when near asymptotic levels ($v''_{\max} = 38$) are included in the data set, and even then its uncertainty is comparable with the *ab initio* calculations (of the order of few percent). The uncertainties in C_8 and C_{10} are larger. When the near asymptotic levels were gradually excluded from the fitted data set, the relative uncertainty of C_6 very soon exceeded 100% ($v''_{\max} = 30$).

In this paper, we are going to examine the extrapolation properties of the CPE potential. The methodology described in [21] is very time consuming, since it is based on fitting thousands of MLR potentials to the experimental frequencies. Therefore, we present a simpler approach here, namely the CPE form will be fitted to the set of points (R_i, U_i) of the same X state potential in Ca_2 as in [13]. We think this is a more efficient way to start the analyses and to draw some important conclusions before the whole machinery from [21] is applied.

2. Chebyshev polynomial expansion potential

In the original paper [10], the CPE potential is defined such that it approaches zero as $R \rightarrow \infty$. Here, we adopted other traditional convention in spectroscopy, namely $U(R_e) = 0$, so to the original definition we have added the energy at the asymptote U_{inf} as follows

$$U(R) = U_{\text{inf}} + \frac{\sum_{k=0}^N c_k T_k(y_p)}{1 + \left(\frac{R}{R_{\text{ref}}}\right)^n}, \quad (3)$$

where

$$y_p = \frac{R^p - R_{\text{ref}}^p}{R^p + R_{\text{ref}}^p - 2R_{\text{min}}^p}. \quad (4)$$

The parameters R_{ref} , R_{min} , n , and p are fixed, T_k are Chebyshev polynomials of the first kind. The fitted parameters are U_{inf} and c_k . In [10], the authors advise R_{ref} to be fixed close the equilibrium distance and R_{min} to be the smallest distance where the potential is intended to be used. In the original paper, it is shown that when $p = 2$ and $n = 6$, the CPE form asymptotically transforms into (1), where the dispersion coefficients are combinations of c_k ,

$$C_6 = -R_{\text{ref}}^6 \sum_{k=0}^N c_k, \quad (5)$$

$$C_8 = 2(R_{\text{ref}}^2 - R_{\text{min}}^2)R_{\text{ref}}^6 \sum_{k=0}^N k^2 c_k. \quad (6)$$

A similar expression exists for C_{10} in [10], however, the signs of long-range coefficients are opposite there, because in the definition of $U_{\text{LR}}(R)$, they appear with positive signs. In the same paper, the authors demonstrate a fit to the experimental energy levels of the Be_2 ground state. There, (5) and (6) were used to limit the variation of c_k by constraining the dispersion coefficients close to their *ab initio* values. This is always a winning strategy when reliable theoretical calculations exist. In this study, however, we will study unconstrained fits of all c_k and will examine whether (5) and (6) can converge to reasonable values for C_6 and C_8 . In other words, we will test whether the build-in asymptotic behavior in the CPE may be used to determine C_6 , C_8 , and U_{inf} .

3. Methodology

As an input data we use an equidistant set of 200 points ($3.6 \leq R \leq 25 \text{ \AA}$) generated from the point-wise potential for the Ca_2 X state [13]. The number of points should be large enough to correctly represent the shape of the potential, both in short- and

TABLE I

Values for U_{inf} [cm^{-1}] and their uncertainties, averaged over the successful fits. The ‘‘true’’ value from [13] is $1102.06(1) \text{ cm}^{-1}$.

N	$R \in [3.6, 10]$ [\AA]	$R \in [3.6, 15]$ [\AA]	$R \in [3.6, 21]$ [\AA]
10	1102.40(120)	1102.30(8)	1102.13(3)
11	1103.40(140)	1102.24(7)	1102.11(3)
12	1104.10(200)	1102.17(10)	1102.08(3)
13	1102.80(330)	1102.07(15)	1102.06(2)
14	1102.20(430)	1102.08(14)	1102.06(3)
15	1102.08(291)	1102.09(21)	1102.06(3)

the long-range regions. Points from the repulsive branch (R smaller than 3.6 \AA) are intentionally not included, because their values are much less certain, and we want to avoid the results from the present test to be influenced by them. The original potential consists of a short range cubic-spline section (for $R < 9.44 \text{ \AA}$) and a pure long range extension (1) for $R \geq 9.44 \text{ \AA}$ with $U_{\text{inf}} = 1102.06 \text{ cm}^{-1}$, $C_6 = 1.0023 \times 10^7 \text{ \AA}^6/\text{cm}$, $C_8 = 3.8 \times 10^8 \text{ \AA}^8/\text{cm}$, and $C_{10} = 5.1 \times 10^9 \text{ \AA}^{10}/\text{cm}$. This potential is able to reproduce all experimental data from [13] within their uncertainty (about 0.01 cm^{-1}). The highest energy levels have $v'' = 38$, and their outermost classical turning points lie at about 20 \AA . The choice of points reflects the R values covered by the experimental data, but we believe this does not influence the main conclusions from this study. What is important is that we are certain of the values of U_i in the short-range at least to within $\pm 0.05 \text{ cm}^{-1}$ and we have a pure long-range function beyond 9.44 \AA . In [13], the uncertainties of the fitted long-range parameters were estimated to be 0.01 cm^{-1} for U_{inf} and $0.033 \times 10^7 \text{ \AA}^6/\text{cm}$ for C_6 . For C_8 , the uncertainty is about $1 \times 10^8 \text{ \AA}^8/\text{cm}$.

The calculated points were fitted by the CPE form (3) with $p = 2$, $n = 6$. The parameters are: $N \in [10, 15]$, $R_{\text{ref}} \in [4.0, 4.6] \text{ \AA}$, and $R_{\text{min}} \in [2.5, 3.1] \text{ \AA}$. In this way, we have ensured the proper long-range behavior and allowed for reasonably wide variation of the fixed parameters.

For every N , a total of 100 CPE potentials were fitted by generating random values for R_{ref} and R_{min} within the given intervals. In each fit, the original data set (R_i, U_i) was modified by adding to each U_i a random shift with a standard deviation $\sigma_i = 0.05 \text{ cm}^{-1}$. This way the spread of the fitted parameters will account for the uncertainties in U_i . The whole procedure was repeated for three data sets: $R \in [3.6, 10] \text{ \AA}$, $R \in [3.6, 15] \text{ \AA}$, and $R \in [3.6, 21] \text{ \AA}$. The fit was considered successful if the dimensionless standard deviation

$$\bar{\sigma} = \sqrt{\frac{1}{m} \sum_{i=1}^m \left(\frac{U_i^{\text{exp}} - U_i^{\text{fit}}}{\sigma_i} \right)^2} \quad (7)$$

TABLE II

Values for $C_6 \times 10^7$ [$\text{\AA}^6/\text{cm}$] and their uncertainties averaged over the successful fits. The “true” value from [13] is $C_6 = 1.003(33) \times 10^7 \text{ \AA}^6/\text{cm}$.

N	$R \in [3.6, 10]$ [\AA]	$R \in [3.6, 15]$ [\AA]	$R \in [3.6, 21]$ [\AA]
10	2.8(15)	2.3(3)	1.7(3)
11	3.4(21)	2.0(4)	1.5(4)
12	6.0(47)	1.5(7)	1.1(5)
13	1.6(80)	0.6(12)	0.8(6)
14	0.5(107)	1.0(14)	0.8(5)
15	0.7(60)	1.0(12)	0.7(7)

TABLE III

Values for $C_8 \times 10^8$ [$\text{\AA}^8/\text{cm}$] and their uncertainties averaged over the successful fits. The “true” value from [13] is $C_8 = 3.8(10) \times 10^8 \text{ \AA}^8/\text{cm}$.

N	$R \in [3.6, 10]$ [\AA]	$R \in [3.6, 15]$ [\AA]	$R \in [3.6, 21]$ [\AA]
10	-51(38)	-37(11)	-22(10)
11	-75(59)	-27(14)	-11(15)
12	144(152)	-6(27)	4(16)
13	6(268)	30(55)	19(18)
14	36(370)	11(70)	19(27)
15	18(214)	9(117)	21(41)

did not exceed 1.5. Actually, only when $N = 10$, the number of successful fits was 95–98. For $N > 10$, all 100 fits were successful.

The computer routine to realize the above mentioned ideas was written in Python. We used the numpy linalg.svd function to optimize the fitted parameters in a least-squares-approximation sense. One of the great advantages of the CPE model is that it is linear with respect to the fitted parameters. Therefore, all fits converged within few iterations. The calculations for one interval (a total of 500 fits) took few minutes on a decent computer.

4. Results

The mean values of the collected U_{inf} , C_6 , and C_8 and their standard deviations are summarized in Tables I–III. Values for C_{10} were also calculated, but their uncertainties were so large that we have omitted them in the tables. In general, the estimated uncertainties grow with the number of c_k parameters — a sign of increasing correlations between fitted parameters.

The values of the dissociation energy U_{inf} (Table I) agree quite well with the original value of $1102.06(1) \text{ cm}^{-1}$. One should keep in mind that for the first interval $R \in [3.6, 10] \text{ \AA}$, only a tiny part of the fitted points belongs to the long-range region ($R > 9.44 \text{ \AA}$). For information, $U(R = 10 \text{ \AA}) \approx 1088 \text{ cm}^{-1}$ and corresponds to $v'' = 32$. When the fitted interval extends further into the long-range region, the fitted U_{inf} approaches the “true” value. For the third interval, apparently, the correlation with the c_k parameters is almost broken, since the uncertainty remains independent of the number of parameters N . However, models with $N = 10$ –12 are not flexible enough and give slightly overestimated predictions.

The situation with the dispersion coefficients is quite different. In general, the uncertainties for C_6 and C_8 are huge. The values for the leading

long-range coefficient (Table II) seem to have reasonable uncertainties only for $R \in [3.6, 21] \text{ \AA}$. They are an order of magnitude larger than those from [13], but a direct comparison is not correct since there the uncertainty is based on the experimental errors of the measured line frequencies, whereas here on the $\pm 0.05 \text{ cm}^{-1}$ uncertainty of the potential points U_i . The goal of the present study is not to compare the two models, but to draw general conclusions of the extrapolation properties of the CPE form. Contrary to the value of U_{inf} , we cannot observe with confidence that the obtained C_6 values converge to the “true” one when the R -interval or N is increased. One can see that C_6 systematically decreases with N , so the correlation between C_6 and c_k is still strong. It might be broken by even larger intervals of R , but such cases are beyond the scope of our study, since we examine the extrapolation properties of CPE, and the interval $R > 21 \text{ \AA}$ is already outside the experimental data.

It seems to be impossible to obtain a reasonable value for C_8 . In [13], its relative uncertainty was also significantly larger than that of C_6 . Here, however, it is almost always larger than 100%. The correlation with C_6 from Table II is visible — larger C_6 are combined with larger and negative C_8 .

The simulations show that despite the built-in long-range form, by fitting the CPE form to data points which (for $R \geq 9.44 \text{ \AA}$) follow exactly the long-range expression (1), we cannot retrieve the “true” dispersion coefficients. To assess where the long-range expression (1) becomes valid for the CPE potentials, in Fig. 2 we plotted six of the fitted CPE potentials (with $N = 15$, fitted in the interval $R \in [3.6, 15] \text{ \AA}$) together with the long-range potentials (1) with parameters C_6 , C_8 , and C_{10} calculated from the fitted c_k as shown in [10] and U_{inf} from the fit. It is clear that the CPE potentials indeed converge to (1), but this happens at too large internuclear distances.

We also performed calculations with 0.01 cm^{-1} noise on data points in the largest interval $R \in [3.6, 21] \text{ \AA}$. This corresponds to a very optimistic estimation of the accuracy of the

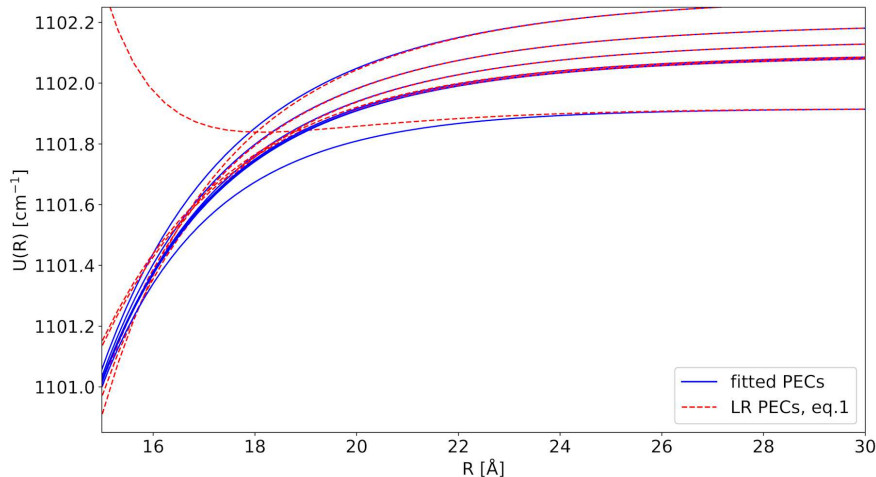


Fig. 2. Fitted CPE potentials with 15 coefficients c_k (blue line) compared with the long-range part (1), where dispersion coefficients are calculated from the fitted c_k values according to [10].

experimental points, especially for larger R . As expected, the values for U_{inf} for $N = 13$ – 16 become $1102.06(1) \text{ cm}^{-1}$, which is in excellent agreement with [13]. However, for C_6 the calculations led to values in the interval $(0.7(3)$ – $0.8(2)) \times 10^7 \text{ Å}^6/\text{cm}$. These results are still in agreement with [13], but systematically lower. The results for C_8 $(20(9)$ – $25(14)) \times 10^8 \text{ Å}^8/\text{cm}$ — higher than in [13] — are also expected to compensate for the smaller C_6 .

5. Conclusions

To determine the long-range coefficients from a limited range of internuclear distances, one definitely needs data at large R , where only the leading term dominates the PECs. This will allow to fix its value and, as a consequence, the values of the higher power coefficients. It seems to us that in the case of CPE, the experimental data did not cover large enough R -range for this to happen. Of course, it is possible to fix the value of C_6 and/or C_8 according to the theoretical predictions, which are usually accurate within a few percent (at least for C_6). This will immediately improve the values of the other fitted coefficients. A similar approach was adopted in the original work [10]. We believe that using the theoretical dispersion coefficients is always a good starting point, unless detailed analyses show that they can be improved by fits of experimental data. Based on the presented simulations, the CPE form cannot be used in such analyses, because the long-range form is achieved at too large R .

Actually, there are few examples in the literature where dispersion coefficients have been determined purely experimentally. None of them, to our best knowledge, uses a single analytic potential function with built-in long-range behavior. At the moment,

the MLR function [19] seems to be the most suitable [21], but there is still room for improvement. Based on our experience so far, we think that the desired analytic form should be simple, should ensure smooth transition to the long-range expression at distances about the Le Roy radius [18], and all other contributions to the potential should approach zero beyond R_{LR} exponentially, as the asymptotic expression for the exchange energy suggests [22].

Of course, depending on the accuracy of the experimental data, the simple form (1) may be enriched with higher power terms, exchange terms [13, 22], or damping functions [23], to account for the part of the potential not entirely in the pure long-range region. For data very close to the asymptote (very large R), one may need to include retardation corrections [24]. However, adding more parameters to the model can increase the correlations between them. Therefore a good practice is to extend the model only when the experimental data are sensitive to the new parameters.

Acknowledgments

The authors acknowledge partial support from the Bulgarian National Science Fund through grant KII-06-H68/30.11.2022. AP acknowledges partial support from the Bulgarian national plan for recovery and resilience, contract BG-RRP-2.004-0008-C01 (SUMMIT), project number 3.1.4.

References

- [1] R. Rydberg, *Z. Phys.* **73**, 376 (1932).
- [2] O. Klein, *Z. Phys.* **76**, 226 (1932).

- [3] A.L.G. Rees, *Proc. Phys. Soc.* **59**, 998 (1947).
- [4] W. Kosman, J. Hinze, *J. Mol. Spectrosc.* **56**, 93 (1975).
- [5] C. Vidal, H. Scheingraber, *J. Mol. Spectrosc.* **65**, 46 (1977).
- [6] P.G. Hajigeorgiou, R.J. Le Roy, *J. Chem. Phys.* **112**, 3949 (2000).
- [7] C. Samuelis, E. Tiesinga, T. Laue, M. Elbs, H. Knöckel, E. Tiemann, *Phys. Rev. A* **63**, 012710 (2000).
- [8] A. Pashov, W. Jastrzębski, P. Kowalczyk, *Comput. Phys. Commun.* **128**, 622 (2000).
- [9] J.Y. Seto, R.J. Le Roy, J. Vergés, C. Amiot, *J. Chem. Phys.* **113**, 3067 (2000).
- [10] V.V. Meshkov, A.V. Stolyarov, M.C. Heaven, C. Haugen, R.J. Le Roy, *J. Chem. Phys.* **140**, 064315 (2014).
- [11] R.J. Le Roy, *J. Quant. Spectrosc. Rad. Trans.* **186**, 179 (2017).
- [12] J.A. Coxon, P.G. Hajigeorgiou, *J. Chem. Phys.* **132**, 094105 (2010).
- [13] O. Allard, C. Samuelis, A. Pashov, H. Knöckel, E. Tiemann, *Eur. Phys. J. D* **26**, 155 (2003).
- [14] A. Pashov, W. Jastrzębski, V. Bednarska, W. Jaśniecki, P. Kowalczyk, *J. Mol. Spectrosc.* **203**, 264 (2000).
- [15] A. Pashov, W. Jastrzębski, P. Kowalczyk, *J. Chem. Phys.* **113**, 6624 (2000).
- [16] A. Pashov, W. Jastrzębski, P. Kowalczyk, *J. Phys. B: At. Mol. Opt. Phys.* **33**, L611 (2000).
- [17] R.J. Le Roy, R.B. Bernstein, *Chem. Phys. Lett.* **5**, 42 (1970).
- [18] R.J. Le Roy, *Can. J. Phys.* **52**, 246 (1974).
- [19] R.J. Le Roy in: *Equilibrium Structures of Molecules*, Ch. 6, Eds. J. Demaison, J.E. Boggs, A.G. Csaszar, Taylor and Francis, London 2011.
- [20] R.J. Le Roy, R.D.E. Henderson, *Mol. Phys.* **105**, 663 (2007).
- [21] A. Sinanaj, A. Pashov, *J. Mol. Spectrosc.* **396**, 111811 (2023).
- [22] S.H. Patil, K.T. Tang, in: *Asymptotic Methods in Quantum Mechanics*, Springer Series in Chemical Physics, Vol. 64, Springer, Berlin 2000.
- [23] K.T. Tang J.P. Toennies, *J. Chem. Phys.* **80**, 3726 (1984).
- [24] E. Pachomow, V.P. Dahlke, E. Tiemann, F. Riehle, U. Sterr, *Phys. Rev. A* **95**, 043422 (2017).